Dynamical Disentangling and Cooling of Atoms in Bilayer Optical Lattices

A. Kantian, S. Langer, and A. J. Daley

Dynamical disentangling and cooling of atoms in bilayer optical lattices

A. Kantian,[1, 2] S. Langer,[3] and A. J. Daley[4]

[1] Nordita, KTH Royal Institute of Technology and Stockholm University,
Roslagstullsbacken 23, SE-106 91 Stockholm Sweden
[2] Department of Physics and Astronomy, Uppsala University, Box 516, S-751 20 Uppsala, Sweden
[3] Department of Physics and Astronomy, University of Pittsburgh, Pittsburgh, Pennsylvania 15260, USA
[4] Department of Physics and SUPA, University of Strathclyde, Glasgow G4 0NG, UK

(Dated: November 30, 2017)

We show how experimentally available bilayer lattice systems can be used to prepare quantum many-body states with exceptionally low entropy in one layer, by dynamically disentangling the two layers. This disentangling operation moves one layer - subsystem A - into a regime where excitations in A develop a single-particle gap. As a result, this operation maps directly to cooling for subsystem A, with entropy being shuttled to the other layer. For both bosonic and fermionic atoms, we study the corresponding dynamics showing that disentangling can be realised cleanly in ongoing experiments. The corresponding entanglement entropies are directly measurable with quantum gas microscopes, and as a tool for producing lower-entropy states, this technique opens a range of applications beginning with simplifying production of magnetically ordered states of bosons and fermions.

Understanding entanglement in many-body systems [1, 2] provides a new way to study various phenomena, from identifying topological states [3–6] to characterizing out-of-equilibrium quench dynamics and fundamental issues such as thermalisation [7, 8]. Entanglement measures in many-body systems can be directly accessed in experiments, as was recently demonstrated for Rényi entropies of itinerant atoms in an optical lattice [9–11]. In the present work, we show how dynamical manipulation of entanglement for atoms in bilayer optical lattices could be used to address a key experimental challenge: based on processes that result in a dynamical disentangling of two layers within a bilayer optical lattice at low temperatures, as shown in Fig. 1, it is possible to transfer most thermal entropy into one of the two layers. Further adiabatic manipulation of the low-entropy layer then makes a broad range of presently unachievable low-temperature phenomena accessible. The required control over the lattice potential is readily available in experiments with optical superlattices [12, 13] or quantum gas microscopes [14].

The first milestone in this direction would be the simplified preparation of quantum magnetic ordering driven by super-exchange processes, which is challenging due to the small energy gaps involved [15–17]. Seminal recent experiments detecting anti-ferromagnetic (AF) correlations for atoms in optical lattices [18, 19] demonstrated entropies within a factor of two of that required for the Néel transition. Further progress was made with individual site addressing in quantum gas microscopes [20–23], revealing magnetic correlations in 2D. However, with the eventual goal of observing effects that require much lower temperatures still [24, 25], it is imperative to develop new ways to strongly reduce the entropy. We show below that our scheme could reduce entropies by more than an or-
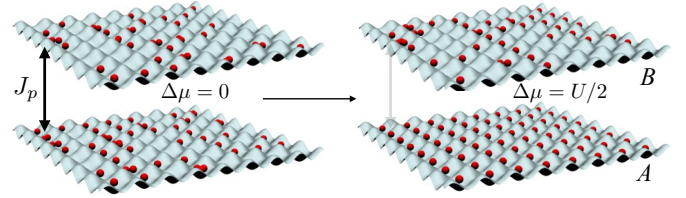

FIG. 1: (Color online) Dynamical disentangling in bilayer systems: the example of single-component bosons: (a) Two tunnel-coupled layers (with interlayer tunnelling J_p) are prepared at the same chemical potential (identical trap depths in the vertical direction). Particles are delocalised between the layers, which are entangled at zero temperature. By manipulating the relative trap depth of the layers, then removing the tunnel coupling, layer A can be prepared in a Mott-insulating state. Having a gapped state in layer A strongly suppresses entanglement of the two layers at zero temperature. At nonzero temperatures, entropy per particle is much higher in layer B, where atoms are free to move.

der of magnitude starting from initial states attainable in current experiments.

Below we first provide a comprehensive explanation of dynamical disentangling, with examples in low-entropy state preparation for single or multi-component bosons with gapped excitation spectra, the latter of which are especially relevant for the study of magnetic ordering in ultracold atomic lattice gases [15, 26–30]. We then discuss combining this scheme with further adiabatic ramps, allowing applications to ungapped systems, with examples from two-component fermions.

A bilayer setup for dynamical disentangling – Here we introduce the concept of dynamical disentangling of two subsystems by considering bosons in a bilayer optical lattice, shown schematically in Fig. 1. For atoms in the

lowest Bloch bands in each layer, under well-controlled approximations the Hamiltonian is a (multi-component) Bose-Hubbard model [31–33], $H = H_A + H_B + H_c$, where ($\hbar \equiv 1$)

$$H_X = -\sum_{\langle l,k\rangle,\sigma} J_\sigma b_{l\sigma X}^\dagger b_{k\sigma X} + V\sum_l n_{l\uparrow X}n_{l\downarrow X}$$
$$+ \sum_{l,\sigma=\uparrow,\downarrow} \frac{U_\sigma}{2}n_{l\sigma,X}(n_{l\sigma X}-1)$$
$$H_c(t) = \sum_{l,\sigma}\left[-J_p^\sigma(t)(b_{l\sigma A}^\dagger b_{l\sigma B}+H.c.) - \Delta\mu_\sigma(t)n_{l\sigma A}\right].$$

Here we consider two layers $X \in \{A, B\}$, and up to two components, labelled $\sigma = \uparrow, \downarrow$, corresponding either to separate species or different internal states of the same atomic species. The operator $b_{l\sigma X}^\dagger$ creates a boson on site l and species σ in layer X, $J_p^\sigma(t)$ denotes inter-layer tunnelling and $\Delta\mu_\sigma(t)$ is a global energy shift between the layers. Within each layer, $n_{l\sigma,X} = b_{l\sigma,X}^\dagger b_{l\sigma,X}$, the tunnelling amplitude is J_σ, the onsite interaction within one component is U_σ, and between components is V. We denote time as t, with T used for total times of parameter ramps (linear in t unless specified). Where multiple parameters are ramped separately, we write $T(P)$, where $P \in \{J_p^\sigma, \Delta\mu_\sigma\}, U_\sigma, V$. We first illustrate the scheme using single-component bosons and then extend this to the two-component magnetically ordered case.

Disentangling bilayer systems in the static limit – Choosing the number of particles N to be fewer than the sum of lattice sites of both layers, $M \equiv M_A + M_B$, then for $\Delta\mu = 0$ the zero-temperature ground state will involve atoms delocalised between the two layers. This results in entanglement of the two subsystems corresponding to layers A and B, even for $U = 0$. Thus, even though the total system is in a pure state with entropy $S \equiv -\mathrm{Tr}\{\rho\log\rho\} = 0$, the entropy of the reduced subsystem for layer A, $S_A \equiv -\mathrm{Tr}\{\rho_A\log\rho_A\}$, will be non-zero, $S_A > 0$, where ρ is the density matrix for the whole system and $\rho_A = \mathrm{Tr}_B\{\rho\}$ [9, 34]. We now consider what happens at weak interlayer coupling, $J_p \to 0$. Increasing the difference in chemical potential between the layers, $\Delta\mu$, we can favour the transfer of particles to layer A. As depicted schematically in Fig. 1, and in the mean-field phase diagram (inset of Fig. 2a), for sufficiently large U/J, layer B remains in a superfluid (SF) regime at zero temperature, while A enters a gapped Mott Insulator (MI) regime. At zero temperature, the gap suppresses excitations in layer A, and for $J_p \to 0$, that layer will be in its ground state. Contributions from other states in layer A are suppressed by the excitation gap, and S_A is also suppressed, as mostly just one state of subsystem A contributes to the ground state of the whole system.

At non-zero temperatures, the subsystem entropy per particle S_A/N_A ($N_X \equiv \sum_l\langle n_{l,X}\rangle$) consists of both thermal and entanglement entropy [9, 35]. As an example, we
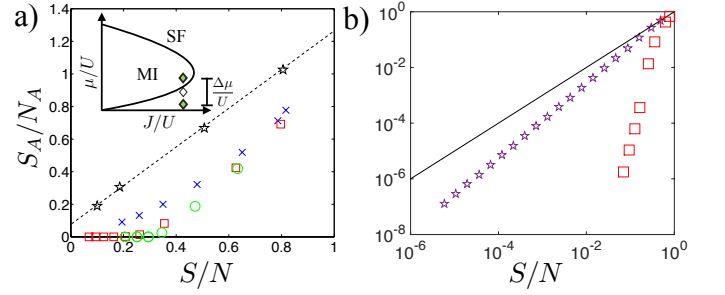

FIG. 2: (Color online). Equilibrium entropies in the limit $J_p, J_p^\sigma \to 0$. (a) Entropy per particle S_A/N_A in layer A of a 1D bilayer system of length 6 with 8 spinless bosons, as a function of total entropy per particle, S/N. Black stars and a fitted dotted line show the case where $U/J = 5$ and $\Delta\mu = 0$, demonstrating non-zero entanglement of the two layers at zero temperature. Remaining points show target parameters for dynamical disentangling, with $\Delta\mu = U/2$. Blue crosses denote $U/J = 8$ ($\beta J \in [0.1, 1.5]$), red squares $U/J = 20$ ($\beta J \in [0.1, 2]$), and green circles $U/J = 50$ ($\beta J \in [0.1, 1]$). For large U/J, S_A/N_A is strongly suppressed for low S/N. Inset: The zero-temperature mean-field phase diagram for the Bose-Hubbard model in the local density approximation, showing two superfluid layers with less than unit filling (central diamond) being separated in chemical potential so that one becomes Mott Insulating and the other remains superfluid (upper and lower diamonds). (b) S_A/N_A of a 1D bilayer system of length 5 with 4 spin-up and 4 spin-down lattice bosons with $U_{\uparrow,\downarrow} \to \infty$, $V = 10J_\downarrow$, as a function of S/N ($\beta J_\downarrow \in [1, 20]$); purple stars). For the parameters . As $J_\uparrow = 3J_\downarrow$, $\Delta\mu_\uparrow = 8.5J_\downarrow$ and $\Delta\mu_\downarrow = 5J_\downarrow$, layer A realizes gapped AF order with exactly 5 bosons with a large charge- and a small spin-gap. Again, S_A/N_A is strongly suppressed at low S/N (see text). For comparison, we show the results from (a) with $U/J = 20$, and plot $S_A/N_A = S/N$ in black. We include maximally 4 bosons per site in our calculations.

calculate this via exact diagonalisation (ED), as shown in Fig. 2a as a function of entropy per particle of the whole system S/N in 1D, with 8 particles in 12 lattice sites ($M_{A,B} = 6$). When S/N is large, layer A is indeed measurably entangled with layer B, but as S/N is reduced, the entropy is almost entirely transferred to layer B, as S_A is strongly suppressed. At zero temperature, $S \to 0$, we see directly the suppression of entanglement between the layers by comparing the black stars, which show S_A for $\Delta\mu = 0$ with the other curves, where $\Delta\mu = U/2$, and $S_A \to 0$ as $S \to 0$. This approach generalizes straightforwardly to two-component bosons with magnetic ordering. Considering a system with $U_\sigma \gg V \gg J_\uparrow > J_\downarrow$ guarantees that both charge and spin excitations of the magnetic order at commensurate filling are gapped [36], which is critical. Calculations (ED) for a system with $M_{A,B} = 5$, $N_{\uparrow,\downarrow} = 4$, $V/J_\downarrow = 10$ $J_\uparrow/J_\downarrow = 3$, show that for the range of $\Delta\mu_\sigma$ corresponding to integer numbers $\langle N_{\sigma,A}\rangle$ and $\langle (N_{\uparrow,A} + N_{\downarrow,A})\rangle = M_A$ an AF order forms in layer A, while S_A is once more strongly suppressed (see Fig. 2b). S_A/N_A is suppressed exponentially with the

size of the smallest gap in subsystem A. We find that S/N and S_A/N_A decay exponentially with inverse temperature for small and moderate temperatures, so that $S_A/N_A \propto (S/N)^{-\gamma}$ (with γ parameter-dependent), as shown in Fig. 2b [37].

The intuitive picture for disentangling requires a non-trivial justification when $J_p, J_p^\sigma \neq 0$. This coupling could conceivably result in long-range correlations in layer A through layer B, such that we no longer have a decoupled MI or AF state. It is of central importance to know whether the coupling along the boundary between the layers can involve exponentially many states at non-vanishing weight, which would result in large entanglement. However, we can show that indeed the resulting entanglement is small [37], as the number of states participating scales *linearly* and *not* exponentially in M_A, and scales to zero with J_p^σ/δ, whenever H_c is local and generates only single-particle excitations in layer A. Here, δ is the smallest gap to single particle excitations in A. This gap is assumed to be finite, even in the thermodynamic limit, in the final state of A. More complex still are questions concerning the dynamics: as the whole system is initially ungapped (and layer B is always ungapped), we need to check whether dynamical ramps can still produce low-entropy states in layer A. In the following, we treat examples of the dynamics that show it is possible to perform these ramps adiabatically at zero temperature for finite systems, and that at non-zero temperature, the vast majority of the entropy is still transferred to layer B even if the ramp is not adiabatic.

Time-dependence of dynamical disentangling – We first investigate the adiabaticity of a ramp with single-component bosons delocalised over two layers into a disentangled state at zero temperature. In Fig. 3a, we plot the final many-body-state fidelities when considering two coupled 1D chains, where dynamics is computable using adaptive time-dependent density matrix renormalization group techniques [38–42]. We see that for relatively short ramps, with a timescale $T \approx 20J^{-1}$, the fidelity $F(T) = |\langle \psi(T)|\psi_{\text{target}}\rangle|^2$ of the final state of the ramp with $J_p \to 0$ and $\Delta\mu = U/2$, ψ_{target} to the time-evolved state $|\psi(T)\rangle$ is almost one.

At non-zero temperatures, the ramp will never be entirely adiabatic. However, if it is sufficiently slow, and the layers can thermalise, we expect that excitations primarily appear in layer B, where they are ungapped, with the gapped final state in layer A still protected. This can be enhanced if we ensure optimal conditions for thermalisation between the layers during the ramp. To demonstrate this, we show in Fig. 3b the final per-particle entropy of layer A, $(S_A/N_A)_{final}$ as a function of the initial per-particle entropy $(S/N)_{initial}$ at finite temperature, for a small system that permits calculations via ED. We note that $(S_A/N_A)_{final}/(S/N)_{initial}$ is strongly suppressed, and that even with the moderate ramp times $\sim 100J^{-1}$, it is possible to obtain $(S_A/N_A)_{final}$ lowered by an or-
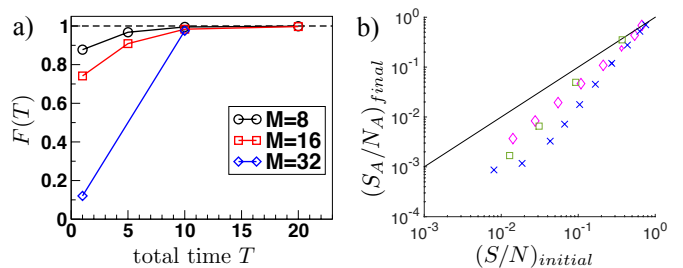

FIG. 3: (Color online) Time-dependent disentangling: (a) At zero temperature, fidelity of the final state of the ramp to the ground state of the system with $\Delta\mu = U/2$, and then to $J_p = 0$, against total ramp time T (measured in units of J^{-1}), computed using t-DMRG techniques for up to $M = 16 \times 2$ lattice sites, always taking $N = 3M/4$ bosons at $U = 8J$. We begin in the ground state with $\Delta\mu = 0$ and $J_p = J$, ramp linearly in time to $\Delta\mu = U/2$, and then to $J_p = 0$. (b) At finite temperature, S_A/N_A at the end of the ramp in 1D bilayer system with $M = 5 \times 2$ for spinless bosons with $N = 7$ and $T = 96J^{-1}$ (blue crosses and magenta diamonds), with $\Delta\mu : 0 \to 10J$ in $T(\Delta\mu) = 92J^{-1}$, followed by $J_p : J \to 0$ within $T(J_p) = 4J^{-1}$. The blue crosses show a ramp with U initially kept at a low constant value $U = J$ for a time $30J^{-1}$, and subsequently $U : J \to 20J$ within $T(U) = 62J^{-1}$. Magenta diamonds show the same protocol, but with $U = 20J$ kept constant throughout. Green squares show the first type of ramp again, but for two-component bosons, $N_{\uparrow,\downarrow} = 4$ and $T = 100J^{-1}$. This ramp into an antiferromagnetic state with gaps to both charge- and spin-excitations uses $J_\uparrow = 3J_\downarrow$, $U_{\uparrow,\downarrow} = \infty$, with $\Delta\mu_\uparrow : 0 \to 8.5J_\downarrow$, $\Delta\mu_\downarrow : 0 \to 5J_\downarrow$ with $T(\Delta\mu_{\uparrow,\downarrow}) = 50J_\downarrow^{-1}$. In parallel, V is kept initially at value $= J_\downarrow$ over timespan $15J_\downarrow^{-1}$, after which $V : J_\downarrow \to 10J_\downarrow$ with $T(V) = 35J_\downarrow^{-1}$. Afterwards, $J_p^\uparrow : 3J_\downarrow \to 0$, $J_p^\downarrow : J_\downarrow \to 0$, with $T(J_p^{\uparrow,\downarrow}) = 50J_\downarrow^{-1}$, thereby accounting for the small gap to spin excitations in layer A. For all shown calculations, maximally 4 bosons per site have been allowed.

der of magnitude over the $(S/N)_{initial}$. Because we expect some degree of non-adiabaticity, the final entropy depends in general on the choice of ramp. We compare two ramps, one with $U/J = 20$ fixed throughout the ramp, and one in which U/J is small initially. The latter case promotes thermalisation between the layers, and results in a substantially lower value for $(S_A/N_A)_{final}$. This strategy can then be repeated, with comparable performance, for spinful bosons to produce magnetically ordered states in layer A, as also depicted in Fig. 3b.

Adiabatically connecting low-entropy disentangled states to broader classes of many-body interacting systems – When the state of the low-entropy layer exhibits a very small (or only finite-size) gap, we can find a related state with a larger gap for dynamical disentangling, and then adiabatically connect this to the final target state. For example, to achieve magnetic ordering for multicomponent bosons and fermions when $J_\uparrow = J_\downarrow$, when there is no spin gap, we can first introduce a
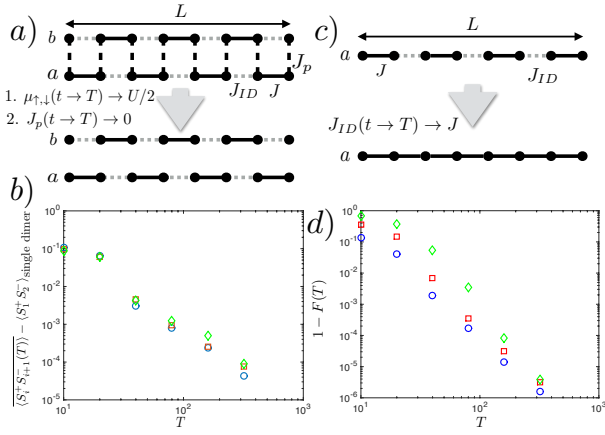
FIG. 4: (Color online) (a) Bilayer disentangling for a dimerised lattice: layers A and B are connected with tunnelling J_p. In each layer, we have alternating tunnelling amplitudes J and J_{ID}. (b) Characterisation of spin singlets produced from fermions on sites with tunnelling J in from (a), with initial parameters $J_p = J$, $J_{ID} = 0$ and $\Delta\mu_{\uparrow,\downarrow} = 0$, ramping to $\Delta\mu_{\uparrow,\downarrow} = U/2$ in time T, then to $J_p = 0$ in time T. We show the difference of the average correlation over all dimers in A $\overline{\langle S_i^+ S_{i+1}^- \rangle}$ at the end of the ramp to the value on a single dimer with one spin-up and spin-down fermion, for system sizes $L = 8$ (blue circles), $L = 16$ (red squares) and $L = 32$ (green diamonds). Here, $U/J = 8$ and $N_\uparrow = N_\downarrow = 3L/4$. (c) Schematic overview of antiferromagnetic state preparation starting from the final state of Fig. 4b (isolated pairs of singlets) and adiabatically increasing tunnelling between dimers. (d) Plot of $1 - F(T)$ for fidelities $F(T)$ at the end of a ramp of timescale T, where J_{1D} is increased from $J_{1D} = 0$ to $J_{1D} = J$, with ramp function $1 - \left(e^{-\nu t} - e^{-\nu T}\right)/(1 - e^{-\nu T})$, $\nu := T/10$. We show results for $U/J = 8$, for system sizes $L = 8$, $L = 16$ and $L = 32$ [symbols as for (b)].

spin gap and then adiabatically remove it in a second step. We give an example for Fermions in the Hubbard model that should simplify the process of achieving these states with low entropies – which are both of acute experimental interest [20–23], and important as starting states for investigating dynamical processes and thermodynamics for systems doped away from half filling.

We again consider spinful Hamiltonians $H = H_A + H_B + H_c$, only now all operators are fermionic, and we assume $J_\uparrow = J_\downarrow$. To have a spin gap opening in layer A in the critical stage in which $\Delta\mu_\sigma$ is ramped to its final non-zero value, we consider the dimerised lattice geometry that was recently realised by Greif et al., [18], and is depicted for a 1D case in Fig. 4a. In equilibrium, Ref. [18] demonstrated the redistribution of entropy with chemical potential, which makes it an excellent candidate for our bilayer disentangling scheme.

In Fig. 4b, we show the schemes efficiency, checking adiabaticity of a chemical potential ramp in this dimerised lattice, analogous to Fig. 3a for bosons. Com-

mencing at less than half filling for the whole system, we produce a half-filled layer A with spin singlets in each dimer. To characterise this final state, we use the local dimer correlation functions as a measure of the final states quality. For all tested system sizes $L = 8$ (blue circles), $L = 16$ (red squares) and $L = 32$ (green diamonds) this scheme exhibits power-law scaling to such low values that it represents near-perfect spin-singlets being prepared on each dimer in layer A. Based on the results of strong-coupling expansions in Ref. [18] and ED calculations, we see that the potential reduction in entropy is similar to that seen for spinful Bosons in Fig. 2b. At current experimental entropies this would allow reductions of the order of a factor of two for easier entry into magnetically ordered states, with much larger reductions possible for lower entropy starting points.

As indicated in Fig. 4c, we then consider the low-entropy layer A, produced above, as a starting point for realising a state with long-range anti-ferromagnetic order by increasing the coupling between dimers time-dependently, analogous to Ref. [43]. Initially one has prepared one up- and one down-spin fermion with $U/J \gg 1$ on each pair of sites with tunnelling amplitude J between them in their ground-state (i.e. the unique singlet state), while inter-dimer tunnelling J_{ID} is at or near zero. Ramping J_{1D} up to J near-adiabatically should result in a smooth crossing over to the desired AF ground state of the Hubbard model at half-filling, as one is initially protected against coupling to excited states by the finite spin-gap. In Fig. 4d we demonstrate that this is the case, plotting one minus the fidelity against the total ramp time after an exponential ramp, (see figure caption). We conclude that the low-entropy dimer state achievable through dynamical disentangling can then be used to prepare a long-range antiferromagnet.

Summary and Outlook –

For realistic experimental timescales and low initial entropies, bilayer disentangling should further suppress the entropy in a single layer by up to an order of magnitude, providing an excellent starting point for adiabatically preparing many-body states. The entropy transfer has advantages over entropy redistribution across a surface [44, 45], as here the inter-layer boundary is equal to the layers in size, and it is easy to isolate the high-entropy layer. This scheme could also be implemented using multiple internal states of atoms rather than spatial bilayer geometries, and the disentangling could be optimised by applying quantum control methods. One can further ask whether dynamical disentangling could work for a wider class of systems, opening formal questions in a quantum information context.

---

[1] L. Amico, R. Fazio, A. Osterloh, and V. Vedral, Rev. Mod. Phys. **80**, 517 (2008).

[2] J. Eisert, M. Cramer, and M. B. Plenio, Rev. Mod. Phys. **82**, 277 (2010).

[3] H.-C. Jiang, Z. Wang, and L. Balents, Nat Phys **8**, 902 (2012).

[4] S. V. Isakov, M. B. Hastings, and R. G. Melko, Nat Phys **7**, 772 (2011).

[5] A. Kitaev and J. Preskill, Phys. Rev. Lett. **96**, 110404 (2006).

[6] M. Levin and X.-G. Wen, Phys. Rev. Lett. **96**, 110405 (2006).

[7] A. M. Kaufman, M. E. Tai, A. Lukin, M. Rispoli, R. Schittko, P. M. Preiss, and M. Greiner, Science **353**, 794 (2016).

[8] M. Rigol, V. Dunjko, and M. Olshanii, Nature **452**, 854 (2008).

[9] R. Islam, R. Ma, P. M. Preiss, M. Eric Tai, A. Lukin, M. Rispoli, and M. Greiner, Nature **528**, 77 (2015).

[10] A. J. Daley, H. Pichler, J. Schachenmayer, and P. Zoller, Phys. Rev. Lett. **109**, 020505 (2012).

[11] C. Moura Alves and D. Jaksch, Phys. Rev. Lett. **93**, 110501 (2004).

[12] S. Folling, S. Trotzky, P. Cheinet, M. Feld, R. Saers, A. Widera, T. Muller, and I. Bloch, Nature **448**, 1029 (2007).

[13] P. J. Lee, M. Anderlini, B. L. Brown, J. Sebby-Strabley, W. D. Phillips, and J. V. Porto, Phys. Rev. Lett. **99**, 020402 (2007).

[14] P. M. Preiss, R. Ma, M. E. Tai, J. Simon, and M. Greiner, Phys. Rev. A **91**, 041602 (2015).

[15] B. Capogrosso-Sansone, Ş. G. Söyler, N. V. Prokof'ev, and B. V. Svistunov, Phys. Rev. A **81**, 053622 (2010).

[16] T.-L. Ho and Q. Zhou, Phys. Rev. Lett. **99**, 120404 (2007).

[17] R. Jördens, L. Tarruell, D. Greif, T. Uehlinger, N. Strohmaier, H. Moritz, T. Esslinger, L. De Leo, C. Kollath, A. Georges, et al., Phys. Rev. Lett. **104**, 180401 (2010).

[18] D. Greif, T. Uehlinger, G. Jotzu, L. Tarruell, and T. Esslinger, Science **340**, 1307 (2013).

[19] R. A. Hart, P. M. Duarte, T.-L. Yang, X. Liu, T. Paiva, E. Khatami, R. T. Scalettar, N. Trivedi, D. A. Huse, and R. G. Hulet, Nature **519**, 211 (2015).

[20] M. Boll, T. A. Hilker, G. Salomon, A. Omran, J. Nespolo, L. Pollet, I. Bloch, and C. Gross, Science **353**, 1257 (2016), ISSN 0036-8075.

[21] M. F. Parsons, A. Mazurenko, C. S. Chiu, G. Ji, D. Greif, and M. Greiner, Science **353**, 1253 (2016), ISSN 0036-8075.

[22] L. W. Cheuk, M. A. Nichols, K. R. Lawrence, M. Okan, H. Zhang, E. Khatami, N. Trivedi, T. Paiva, M. Rigol, and M. W. Zwierlein, Science **353**, 1260 (2016), ISSN 0036-8075.

[23] P. T. Brown, D. Mitra, E. Guardado-Sanchez, P. Schauß, S. S. Kondov, E. Khatami, T. Paiva, N. Trivedi, D. A. Huse, and W. S. Bakr (2016), arXiv:1612.07746.

[24] I. Bloch, J. Dalibard, and S. Nascimbene, Nat Phys **8**, 267 (2012).

[25] J. I. Cirac and P. Zoller, Nat Phys **8**, 264 (2012).

[26] A. B. Kuklov and B. V. Svistunov, Phys. Rev. Lett. **90**, 100401 (2003), ISSN 0031-9007.

[27] A. Isacsson, M.-C. Cha, K. Sengupta, and S. M. Girvin, Phys. Rev. B **72**, 184507 (2005), ISSN 1098-0121.

[28] M. Guglielmino, V. Penna, and B. Capogrosso-Sansone, Phys. Rev. A **84**, 031603 (2011), ISSN 1050-2947.

[29] F. Cattani, C. Gross, M. K. Oberthaler, and J. Ruostekoski, New J. Phys. **15**, 063035 (2013), ISSN 13672630, arXiv:1302.3040v1.

[30] W. Wang, V. Penna, and B. Capogrosso-Sansone, New J. Phys. **18**, 063002 (2016), ISSN 13672630, arXiv:1512.07954v1.

[31] M. Lewenstein, A. Sanpera, and V. Ahufinger, *Ultracold Atoms in Optical Lattices: Simulating quantum many-body systems* (OUP Oxford, 2012).

[32] D. Jaksch and P. Zoller, Annals of Physics **315**, 52 (2005).

[33] D. Jaksch, C. Bruder, J. I. Cirac, C. W. Gardiner, and P. Zoller, Phys. Rev. Lett. **81**, 3108 (1998).

[34] M. R. Dowling, A. C. Doherty, and H. M. Wiseman, Phys. Rev. A **73**, 052323 (2006).

[35] H. Pichler, L. Bonnes, A. J. Daley, A. M. Läuchli, and P. Zoller, New Journal of Physics **15**, 063003 (2013).

[36] E. Altman, W. Hofstetter, E. Demler, and M. D. Lukin, New J. Phys. **5**, 113 (2003), ISSN 1367-2630.

[37] See Supplemental Material at XXX for details.

[38] U. Schollwoeck, Annals of Physics **326**, 96 (2011), ISSN 0003-4916, january 2011 Special Issue.

[39] G. Vidal, Phys. Rev. Lett. **93**, 040502 (2004).

[40] S. R. White and A. E. Feiguin, Phys. Rev. Lett. **93**, 076401 (2004).

[41] A. J. Daley, C. Kollath, U. Schollwöck, and G. Vidal, J. Stat. Mech. p. P04005 (2004).

[42] F. Verstraete, V. Murg, and J. I. Cirac, Adv. Phys. **57**, 143 (2008).

[43] M. Lubasch, V. Murg, U. Schneider, J. I. Cirac, and M.-C. Bañuls, Phys. Rev. Lett. **107**, 165301 (2011).

[44] J.-S. Bernier, C. Kollath, A. Georges, L. De Leo, F. Gerbier, C. Salomon, and M. Köhl, Phys. Rev. A **79**, 061601 (2009).

[45] M. P. Zaletel, D. M. Stamper-Kurn, and N. Y. Yao (2016), 1611.04591.